

***In situ* photoemission study of Nd_{1-x}Sr_xMnO₃ epitaxial thin films**H. Wadati,¹ A. Chikamatsu,² H. Kumigashira,^{2,3,4} A. Fujimori,¹ M. Oshima,^{2,3,4} M. Lippmaa,⁵ M. Kawasaki,⁶ and H. Koinuma⁷¹*Department of Physics, University of Tokyo, Bunkyo-ku, Tokyo 113-0033, Japan*²*Department of Applied Chemistry, University of Tokyo, Bunkyo-ku, Tokyo 113-8656, Japan*³*Core Research for Evolutional Science and Technology of Japan Science and Technology Agency, Chiyoda-ku, Tokyo 102-0075, Japan*⁴*Synchrotron Radiation Research Organization, University of Tokyo, Bunkyo-ku, Tokyo 113-8656, Japan*⁵*Institute for Solid State Physics, University of Tokyo, Kashiwa, Chiba 277-8581, Japan*⁶*Institute for Materials Research, Tohoku University, 2-1-1 Katahira, Aoba, Sendai 980-8577, Japan*⁷*National Institute for Materials Science, 1-1-1 Sengen, Tsukuba, Ibaraki 305-0047, Japan*

(Received 27 October 2008; revised manuscript received 13 March 2009; published 15 April 2009)

We have performed an *in situ* photoemission study of Nd_{1-x}Sr_xMnO₃ (NSMO) thin films grown on SrTiO₃ (001) substrates by laser molecular-beam epitaxy. The lattice constants of the thin films were relaxed from those of the substrates, and the transport properties were almost the same as those of bulk NSMO. From core-level photoemission studies, we found that the behavior of the chemical-potential shift was not much different from that of the bulk NSMO samples. In the valence-band spectra, finite intensity at the Fermi level was observed even in the insulating phase. The band dispersions of Nd_{0.6}Sr_{0.4}MnO₃ obtained by angle-resolved photoemission spectroscopy were almost the same as those of La_{0.6}Sr_{0.4}MnO₃ thin films. These results showed that NSMO is closely related to La_{1-x}Sr_xMnO₃ in terms of the band structure, except for a decrease in the coherent spectral weight.

DOI: [10.1103/PhysRevB.79.153106](https://doi.org/10.1103/PhysRevB.79.153106)

PACS number(s): 71.28.+d, 71.30.+h, 79.60.Dp, 73.61.-r

Hole-doped perovskite manganese oxides R_{1-x}A_xMnO₃, where R is a rare earth (R=La, Nd, Pr) and A is an alkaline-earth atom (A=Sr, Ba, Ca), have attracted much attention because of their remarkable physical properties such as the colossal magnetoresistance and the ordering of spin, charge, and orbitals.¹ Their electronic phase diagram is shown in Ref. 1. La_{1-x}Sr_xMnO₃ (LSMO) has a large bandwidth W, and ferromagnetic metallic (FM) phase is realized between x ≈ 0.2 and 0.5.² Charge-ordered (CO) insulating state is another phase which competes with the FM phase. Most of hole-doped manganites (x ≈ 0.5) with a small W exhibit a so-called charge-exchange “(CE)-type” antiferromagnetic ordering with alternating Mn³⁺ and Mn⁴⁺ sites within the (001) plane.³ Pr_{1-x}Ca_xMnO₃ (PCMO), where W is the smallest, has a particularly stable CO state in a wide hole concentration range between x ≈ 0.3 and 0.75.⁴ Nd_{1-x}Sr_xMnO₃ (NSMO) has an intermediate bandwidth W. In bulk NSMO, the FM state is realized between x ≈ 0.25 and 0.48, and the CO state exists in a very narrow concentration range near x = 0.5.¹

Recently, Wadati *et al.*⁵ studied the electronic structure of PCMO thin films grown on LaAlO₃ (LAO) (001) substrates by photoemission spectroscopy. The PCMO thin films were influenced by compressive strain from the LAO substrates. The photoemission results were quite different from those of PCMO bulk samples⁶ in that the two characteristic behaviors observed in bulk samples, namely, the spectral weight transfer near the Fermi level (E_F) and the suppression of the chemical-potential shift with hole doping, were not observed. They considered it to be spectroscopic evidence for the suppression of incommensurate charge modulation in the PCMO thin films grown on the LAO substrates. Horiba *et al.*⁷ also performed a similar photoemission study of LSMO thin films grown on SrTiO₃ (STO) (001) substrates. In contrast to PCMO thin films on LAO, the differences of the electronic structures between film and bulk² properties were not ob-

served. In this work, we have investigated the electronic structure of NSMO thin films grown on STO (001) substrates. The in-plane lattice constants of the fabricated NSMO thin films were relaxed from those of the STO substrates. From core-level photoemission studies, we found that the behavior of the chemical-potential shift was not much different from that of the bulk NSMO samples.⁸ The band dispersions obtained by angle-resolved photoemission spectroscopy (ARPES) were almost the same as those of LSMO thin films.⁹ These results show that the electronic structure of the NSMO thin films were similar to those of the bulk samples due to the effects of relaxation. The reduction in the bandwidth was not clearly observed in NSMO thin films compared to LSMO, but the decrease in the coherent spectral weight of the e_g band was observed, which explains the reduction in the ferromagnetic transition temperature (T_c) in NSMO compared to LSMO.

The experiments were performed at beamlines 1C and 2C of the Photon Factory, High Energy Accelerators Research Organization (KEK), using a combined laser molecular-beam-epitaxy (MBE) photoemission spectrometer system.¹⁰ Epitaxial thin films of NSMO with a thickness of about 400 Å were fabricated by the pulsed laser deposition method from ceramic targets of desired chemical compositions. Single crystals of STO (001) were used as the substrates. A Nd:YAG (yttrium aluminum garnet) laser was used for ablation in its frequency tripled mode (λ = 355 nm). NSMO thin films were deposited on the substrates at 1050 °C at an oxygen pressure of 1 × 10⁻⁴ Torr. The films were postannealed at 400 °C at an atmospheric pressure of oxygen to remove oxygen vacancies. The samples were transferred from the laser MBE chamber to the spectrometer under an ultrahigh vacuum of 10⁻¹⁰ Torr. Atomically flat step-and-terrace structures were observed by atomic force microscopy. The crystal structure was characterized by four circle x-ray diffraction

TABLE I. Ferromagnetic (T_c) and Néel (T_N) transition temperatures of fabricated NSMO thin films and comparison with bulk values (Ref. 1).

x	T_c or T_N (film) (K)	T_c or T_N (bulk) (K)
0.2	$T_c \sim 130$	$T_c \sim 190$
0.4	$T_c \sim 190$	$T_c \sim 280$
0.55	$T_N \sim 260$	$T_N \sim 230$

measurements. The thin films were found to be relaxed from the substrates, but the lattice constants were not fully relaxed to the bulk values and the films were with in-plane tensile strain effects from STO substrates. For example, the in-plane (a) and out-of-plane (c) lattice constants of NSMO ($x=0.4$) thin films were 3.898 and 3.816 Å, respectively, and the in-plane lattice constant was not the same as that of STO ($a=3.905$ Å). In the low energy electron diffraction patterns, sharp 1×1 spots were observed with some surface-reconstruction-derived superstructure spots. The electrical resistivities were similar to those of the relaxed thin films previously reported.¹¹ From magnetization measurements, the T_c of NSMO ($x=0.4$) thin films was determined to be ~ 190 K, similar to that of the relaxed thin films previously reported¹¹ but lower than that of NSMO bulk samples (~ 280 K) (Ref. 1) and that of LSMO ($x=0.4$) thin films (~ 350 K).⁷ We consider that this difference of T_c comes from in-plane tensile strain effects from STO substrates. At $x=0.2$ and 0.55, NSMO thin films show ferromagnetic and antiferromagnetic behaviors, respectively. We summarize in Table I the transition temperatures of the NSMO films.

The photoemission spectra were taken using a Gamma-data Scienta SES-100 spectrometer. The x-ray absorption spectroscopy (XAS) spectra were measured using the total-electron-yield method. All the spectra were measured at room temperature except for the ARPES measurements (20 K). The total energy resolution was about 150–400 meV depending on photon energies. The E_F position was determined by measuring gold spectra.

Figure 1 shows the core-level photoemission spectra of

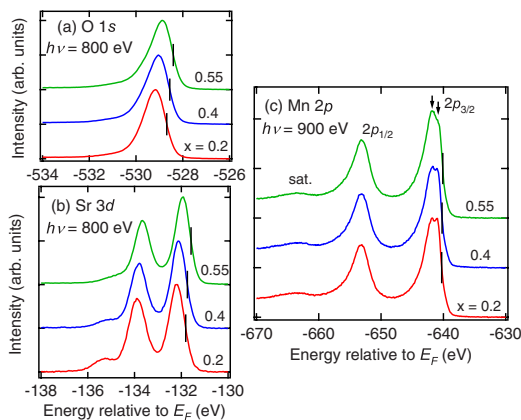


FIG. 1. (Color online) Core-level photoemission spectra of NSMO thin films.

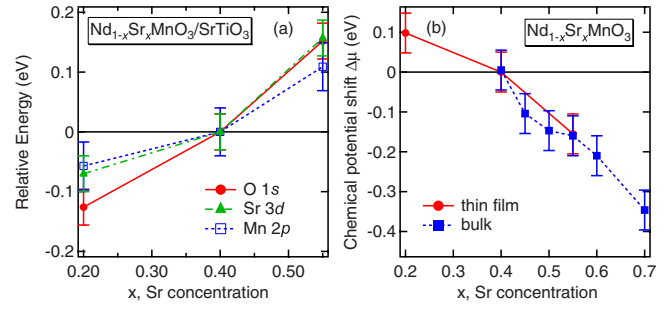


FIG. 2. (Color online) Binding-energy shifts of the core levels in NSMO thin films. (a) Shift of each core level. (b) Chemical-potential shift deduced from the core-level shifts. The results of bulk samples are taken from Ref. 8.

NSMO thin films. The small amount of contamination signal on the higher-binding-energy side of the O 1s peak indicates that the surface was reasonably clean due to the *in situ* measurements. The line shape of the Mn 2p core level had almost no composition dependence; that is, the intensity of the satellite structures and the energy separation between the main peaks and the satellite structures were almost the same for all values of x . There are two structures in Mn 2p_{3/2} peaks, as indicated by arrows in Fig. 1(c), in all compositions ($x=0.2, 0.4, 0.55$), and the relative intensities of these two structures are different in $x=0.55$.

Figure 2(a) shows the binding-energy shifts of core levels as a function of x . The midpoints of the lower-binding-energy slopes are indicated as the bars in Fig. 1, and they are taken as representing the shift of the peaks because this part is generally least affected by possible contamination. Here, the “relative energies” are referenced to the sample of $x=0.4$. Mn 2p moves in the same direction as all the other core levels, in contrast to bulk samples.⁸ This difference of the behavior of Mn 2p has already been observed in LSMO bulk¹² and thin films on STO substrates,⁷ and the origin of this difference is not clear at this moment but probably related to in-plane tensile strain effects from STO substrates. The chemical-potential shift $\Delta\mu$ can be obtained from the average of the energy shifts of the O 1s and Sr 3d core levels.⁸ Figure 2(b) shows $\Delta\mu$ thus determined plotted together with the bulk NSMO results.⁸ The $\Delta\mu$ of thin films is in good agreement with that of bulk samples. In the bulk samples, there is a suppression of $\Delta\mu$ in the narrow composition region around $x=0.5$, that is, $0.45 \leq x \leq 0.55$, corresponding to the narrow region of CO in the phase diagram of NSMO.¹ In the NSMO thin films, long-range CO does not occur on STO (001) substrates but exists on STO (011) substrates.¹³ Our thin films were grown on STO (001), and therefore CO is expected to be absent. Further studies around $x=0.5$ and also on NSMO/STO(011) are necessary to determine whether there is a suppression of $\Delta\mu$ in NSMO thin films.

Figure 3 shows the valence-band photoemission spectra of NSMO ($x=0.4$) thin films taken at three photon energies: 600, 643, and 979 eV. The spectra consist of four main structures labeled as A, B, C, and D. The spectra taken at $h\nu=643$ and 979 eV are Mn 2p-3d and Nd 3d-4f on resonance, respectively. In the Mn 2p-3d on-resonance spectrum, there

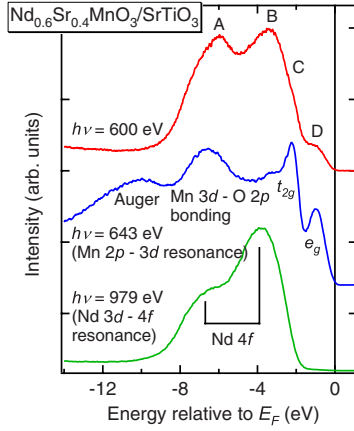


FIG. 3. (Color online) Valence-band photoemission spectra of NSMO ($x=0.4$) thin films taken at various photon energies.

are three structures: Mn $3d e_g$ states, Mn $3d t_{2g}$ states, and Mn $3d$ -O $2p$ bonding states. In the Nd $3d$ - $4f$ on-resonance spectrum, there are two structures of Nd $4f$ characters. Therefore, structures A and B are assigned to Mn $3d$ -O $2p$ bonding and Nd $4f$ -O $2p$ hybridized states, structure C to Mn $3d t_{2g}$ states, and structure D to Mn $3d e_g$ states. A finite intensity at E_F was observed especially in the Mn $2p$ - $3d$ on-resonance spectrum, although this sample was in the insulating phase. T_c is about 190 K in $x=0.4$ thin films, far below room temperature (~ 300 K), so we expect that the system is insulating at room temperature. Therefore, the finite intensity at E_F at room temperature, which has already been reported in bulk samples,¹⁴ is a little surprising result, and this has often been interpreted as the existence of FM fluctuations in the insulating state.

Figure 4 shows the doping dependence of the valence-band photoemission and the O $1s$ XAS spectra. In the photoemission spectra, one can observe four main structures A, B, C, and D as already shown in Fig. 3. The energy positions of these four structures indicated as bars in Fig. 4(a) were determined by taking zero points of the first derivatives (A and B) or minimums of the second derivatives (C and D). Structures A–D move toward E_F upon hole doping in good agreement with the core-level shifts, indicating that a rigid-band shift occurs in the valence band. In addition, structure D, which is assigned to the “ $e_{g\uparrow}$ band” becomes weaker with

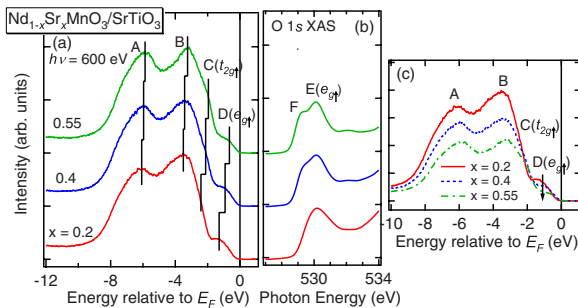


FIG. 4. (Color online) Photoemission and XAS spectra of NSMO thin films. (a) Valence-band photoemission spectra. (b) O $1s$ XAS spectra. (c) Valence-band photoemission spectra normalized to the Nd $4f$ concentrations ($1-x$).

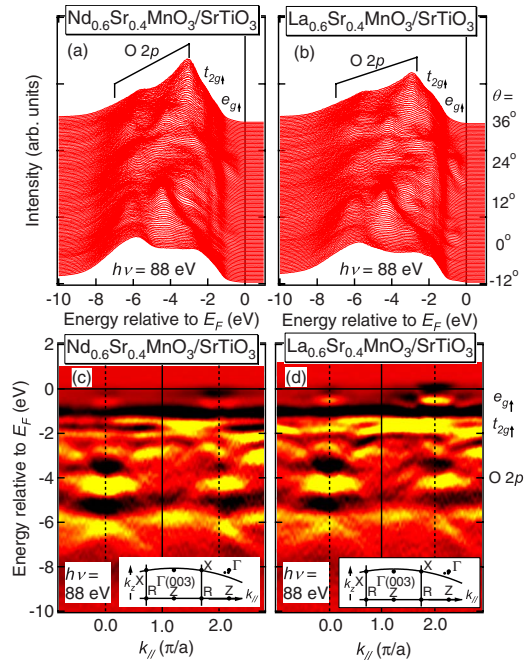


FIG. 5. (Color online) (a) ARPES spectra of NSMO and (b) LSMO (taken from Ref. 9) taken at 88 eV. Panels (c) and (d) show the experimental band structure deduced from the second derivatives of the energy distribution curves. Bright parts correspond to energy bands. The insets show the traces in k space.

increasing x , indicating that holes are doped into the $e_{g\uparrow}$ band. The weakening of structure D with x is more clearly seen in Fig. 4(c), where the spectra have been normalized to Nd $4f$ concentrations ($1-x$). (At 600 eV, the cross-section ratio, including the number of atoms in a unit cell, is Nd $4f$:Mn $3d$:O $2p \sim 4:2:1$, so structures A and B come mainly from Nd $4f$ contributions.) In the O $1s$ XAS spectra in Fig. 4(b), there are two structures labeled as E and F. Structures E and F are assigned to the Mn $3d e_{g\uparrow}$ states.¹⁵ Structure F grows in intensity upon hole doping, indicating that doped holes go into this structure. The photoemission and XAS spectra thus demonstrate that spectral weight is transferred from structure D below E_F to structure F above E_F . This nonrigid-band behavior within ~ 2 eV of E_F appears different from the monotonic chemical-potential shift. Therefore, as in the case of $\text{La}_{1-x}\text{Sr}_x\text{FeO}_3$,²⁰ we conclude that the effect of hole doping can be described in the framework of the rigid-band model as far as the shifts of the spectral features are concerned, whereas the $e_{g\uparrow}$ band shows highly nonrigid-bandlike behavior with spectral weight transfer from below E_F to above it.

Figure 5 shows the ARPES spectra of the (a) NSMO ($x=0.4$) thin film taken with a photon energy of 88 eV, together with the results of the (b) LSMO ($x=0.4$) thin film. This is the first ARPES measurements of NSMO, which has become possible by using thin-film samples prepared *in situ*. The plots of the second derivatives of the energy distribution curves, with bright parts corresponding to energy bands, are shown in panels (c) and (d). The insets show the traces in k space, which are almost along the Γ - X direction due to the uncertainty of the electron momentum perpendicular to the

crystal surface.²¹ The band dispersions of NSMO and LSMO thin films were very similar except for the intensity of the $e_{g\uparrow}$ bands near E_F . As has been discussed in Ref. 9, there is good agreement between ARPES and band-structure calculations based on local density approximation $+U$, except for the renormalization effects of the $e_{g\uparrow}$ bands. The intensity at E_F of NSMO was greatly reduced compared with that of LSMO, although the bottoms of the $e_{g\uparrow}$ bands in these two materials are almost in the same energy position. Lattice constant change between NSMO and LSMO is within $\sim 1\%$, which means that the bandwidth proportional to $\cos^2 \theta$ (θ is a Mn-O-Mn bond angle) does not change so much. The difference in the electronic structure appears as the reduction in the spectral weight of the dispersing (coherent) $e_{g\uparrow}$ bands. The T_c 's are ~ 190 K in NSMO ($x=0.4$) thin films and ~ 350 K in LSMO ($x=0.4$) thin films. This reduction of T_c in NSMO cannot be ascribed to the reduction in the bandwidth, which is too small to be detectable, but to the reduction in the coherent spectral weight. The similar relationship between T_c and coherent spectral weight has also been reported in the ARPES study of LSMO thin films with various T_c 's (Ref. 22) and can be qualitatively explained by the double-exchange theory.

We have performed an *in situ* photoemission study of NSMO thin films grown on STO (001) substrates. From the core-level photoemission study, we found that the behavior of the chemical-potential shift was almost the same as that of

the bulk samples. In the valence-band spectra, we found that there was a finite intensity at E_F even in the insulating phase, and transfer of spectral weight occurred across E_F with hole doping. We also performed ARPES measurements of the NSMO thin films, which became possible by using thin-film samples prepared *in situ*. The band dispersions obtained by ARPES were almost the same as those of LSMO thin films. These results are almost the same as the previous results of bulk samples^{8,14} and surely demonstrate that the electronic structure of the NSMO thin films on STO substrates was almost the same as the bulk samples due to the effects of relaxation. The reduction in the ferromagnetic transition temperature compared to LSMO cannot be ascribed to the decrease in the bandwidth but to the decrease in the coherent spectral weight of the e_g band.

The authors are grateful to K. Ono and A. Yagishita for their support at KEK-PF. This work was supported by a Grant-in-Aid for Scientific Research (Grant No. A19204037, No. A19684010, and No. B19340094) from the Japan Society for the Promotion of Science (JSPS) and a Grant-in-Aid for Scientific Research in Priority Areas "Invention of Anomalous Quantum Materials" from the Ministry of Education, Culture, Sports, Science and Technology. H.W. acknowledges financial support from JSPS. The work was done under the approval of the Photon Factory Program Advisory Committee (Proposals No. 2005G101 and No. 2005S2-002) at the Institute of Material Structure Science, KEK.

¹Y. Tokura, Rep. Prog. Phys. **69**, 797 (2006).

²A. Urushibara, Y. Moritomo, T. Arima, A. Asamitsu, G. Kido, and Y. Tokura, Phys. Rev. B **51**, 14103 (1995).

³Z. Jirák, S. Krupička, V. Nekvasil, E. Pollert, G. Villeneuve, and F. Zounová, J. Magn. Magn. Mater. **15-18**, 519 (1980).

⁴Y. Tomioka, A. Asamitsu, H. Kuwahara, Y. Moritomo, and Y. Tokura, Phys. Rev. B **53**, R1689 (1996).

⁵H. Wadati, A. Maniwa, A. Chikamatsu, I. Ohkubo, H. Kumigashira, M. Oshima, A. Fujimori, M. Lippmaa, M. Kawasaki, and H. Koinuma, Phys. Rev. Lett. **100**, 026402 (2008).

⁶K. Ebata, H. Wadati, M. Takizawa, A. Fujimori, A. Chikamatsu, H. Kumigashira, M. Oshima, Y. Tomioka, and Y. Tokura, Phys. Rev. B **74**, 064419 (2006).

⁷K. Horiba, A. Chikamatsu, H. Kumigashira, M. Oshima, N. Nakagawa, M. Lippmaa, K. Ono, M. Kawasaki, and H. Koinuma, Phys. Rev. B **71**, 155420 (2005).

⁸K. Ebata, M. Takizawa, A. Fujimori, H. Kuwahara, Y. Tomioka, and Y. Tokura, Phys. Rev. B **78**, 020406(R) (2008).

⁹A. Chikamatsu, H. Wadati, H. Kumigashira, M. Oshima, A. Fujimori, N. Hamada, T. Ohnishi, M. Lippmaa, K. Ono, M. Kawasaki, and H. Koinuma, Phys. Rev. B **73**, 195105 (2006).

¹⁰K. Horiba, H. Oguchi, H. Kumigashira, M. Oshima, K. Ono, N. Nakagawa, M. Lippmaa, M. Kawasaki, and H. Koinuma, Rev. Sci. Instrum. **74**, 3406 (2003).

¹¹M. Kasai, H. Kuwahara, Y. Moritomo, Y. Tomioka, and Y. Tokura, Jpn. J. Appl. Phys., Part 2 **35**, L489 (1996).

¹²J. Matsuno, A. Fujimori, Y. Takeda, and M. Takano, Europhys. Lett. **59**, 252 (2002).

¹³M. Nakamura, Y. Ogimoto, H. Tamaru, M. Izumi, and K. Miyano, Appl. Phys. Lett. **86**, 182504 (2005).

¹⁴A. Sekiyama, H. Fujiwara, A. Higashiya, S. Imada, H.

Kuwahara, Y. Tokura, and S. Suga, arXiv:cond-mat/0401601 (unpublished).

¹⁵Dessau *et al.* (Ref. 16) confirmed this assignment by measuring polarization-dependent XAS spectra. This is also supported by the fact that the $t_{2g\downarrow}$ states should have a low intensity because of the weak hybridization between the O $2p$ and Mn $t_{2g\downarrow}$ states. However, there are some papers which claim that structures E and F are assigned to the Mn $3d t_{2g\downarrow}$ and $e_{g\uparrow}$ states, respectively, (Refs. 17 and 18) and there is still controversy (Ref. 19).

¹⁶D. S. Dessau, Y. D. Chuang, A. Gromko, T. Saitoh, T. Kimura, and Y. Tokura, J. Electron Spectrosc. Relat. Phenom. **117-118**, 265 (2001).

¹⁷E. Pellegrin, L. H. Tjeng, F. M. F. de Groot, R. Hesper, G. A. Sawatzky, Y. Moritomo, and Y. Tokura, J. Electron Spectrosc. Relat. Phenom. **86**, 115 (1997).

¹⁸J.-H. Park, T. Kimura, and Y. Tokura, Phys. Rev. B **58**, R13330 (1998).

¹⁹N. Mannella, A. Rosenhahn, M. Watanabe, B. Sell, A. Nambu, S. Ritchey, E. Arenholz, A. Young, Y. Tomioka, and C. S. Fadley, Phys. Rev. B **71**, 125117 (2005).

²⁰H. Wadati, D. Kobayashi, H. Kumigashira, K. Okazaki, T. Mizokawa, A. Fujimori, K. Horiba, M. Oshima, N. Hamada, M. Lippmaa, M. Kawasaki, and H. Koinuma, Phys. Rev. B **71**, 035108 (2005).

²¹H. Wadati, T. Yoshida, A. Chikamatsu, H. Kumigashira, M. Oshima, H. Eisaki, Z.-X. Shen, T. Mizokawa, and A. Fujimori, Phase Transitions **79**, 617 (2006).

²²M. Shi, M. C. Falub, P. R. Willmott, J. Krempasky, R. Herger, L. Patthey, K. Hricovini, C. V. Falub, and M. Schneider, J. Phys.: Condens. Matter **20**, 222001 (2008).